



## Molecular Crystals and Liquid Crystals Science and Technology. Section A. Molecular Crystals and Liquid Crystals

Publication details, including instructions for authors and subscription information:

<http://www.tandfonline.com/loi/gmcl19>

## Liquid Crystal Displays and Novel Optical Thin Films Enabled by Photo-Alignment

Martin Schadt<sup>a</sup>

<sup>a</sup> ROLIC Research Ltd, 4123, Allschwil, Switzerland

Version of record first published: 24 Sep 2006

To cite this article: Martin Schadt (2001): Liquid Crystal Displays and Novel Optical Thin Films Enabled by Photo-Alignment, Molecular Crystals and Liquid Crystals Science and Technology. Section A. Molecular Crystals and Liquid Crystals, 364:1, 151-169

To link to this article: <http://dx.doi.org/10.1080/10587250108024985>

PLEASE SCROLL DOWN FOR ARTICLE

Full terms and conditions of use: <http://www.tandfonline.com/page/terms-and-conditions>

This article may be used for research, teaching, and private study purposes. Any substantial or systematic reproduction, redistribution, reselling, loan, sub-licensing, systematic supply, or distribution in any form to anyone is expressly forbidden.

The publisher does not give any warranty express or implied or make any representation that the contents will be complete or accurate or up to

date. The accuracy of any instructions, formulae, and drug doses should be independently verified with primary sources. The publisher shall not be liable for any loss, actions, claims, proceedings, demand, or costs or damages whatsoever or howsoever caused arising directly or indirectly in connection with or arising out of the use of this material.

## **Liquid Crystal Displays and Novel Optical Thin Films Enabled by Photo-Alignment**

MARTIN SCHADT

*ROLIC Research Ltd, 4123 Allschwil, Switzerland*

Photo-alignment and photo-patterning of monomeric- and polymeric liquid crystals by the linear photo-polymerisation (LPP) technology enables novel molecular configurations in liquid crystal displays (LCDs) as well as a plethora of new thin-film optical elements on single plastic substrates. A molecular building block design of LPP photo-co-polymers with display-specific functional groups is depicted. Contrast and brightness of twisted nematic (TN)-LCDs are shown to markedly improve by combining photo-aligned multi-domain TN-LC-configurations with liquid crystal polymer (LCP) wide-view films. To illustrate the diversity of the LPP/LCP technology, the following photo-aligned new optical thin-film elements on plastic films are presented; colorless nematic wide-view films for TN-LCDs, ideally bright polarisation interference color filters which meet PAL/SECAM standards, as well as photo-aligned and photo-patterned linear polarizers. Photo-generated monomer and polymer liquid crystal devices are key to enable future complex plastic LCDs.

**Keywords:** Liquid crystal displays; photo-alignment; liquid crystal polymers; wide-view optical films; interference color filters; linear polarizers

## 1. Introduction

The director configuration  $\hat{n}$  in the liquid crystal (LC) layer of any field-effect liquid crystal display (LCD) must be unambiguously defined under any driving condition. To achieve this, the azimuthal directions  $\varphi$  and the bias tilt angles  $\Theta$  of the alignment  $\hat{n}(\Theta, \varphi)$  of the configuration at the respective display boundaries must meet the requirements of the electro-optical effect on which the display is based. Effect-specific boundary conditions are prerequisite to achieve the desired voltage-controlled optical retardation and the proper states of polarization of an LCD. As a consequence, this enables dislocation-free, reversible deformation of the configuration under electric fields and therefore uniform display appearance. The basic performance of a display, i.e. its appearance without additional means to improve the optics, is determined by the effect-specific configuration of the LC-molecules. The optical appearance of different effects varies considerably; only a few can be used without effect-specific correction elements.

All LC-configurations assume director configurations – either in their on- or off-states, or under intermediate driving conditions – leading to viewing angle dependent polarization states. The degree varies among different configurations. As a result, contrast, gray scale, color and brightness of displayed images are affected. The strongest angular dependencies occur in displays with planar- to homeotropic director transitions between switching states, whereas in-plane switched LC-configurations are less prone to viewing angle variations. For example, a homeotropically aligned LC-layer is optically uniaxial for vertically incident light. Therefore, it appears black in the off-state between crossed polarizers at vertical light incidence, limited only by the polarizer quality. However, at non-vertical light incidence the vertical black state turns into strongly angular dependent gray states due to the apparent tilted director configuration.

Reflective and transmissive LCDs can be treated as systems which consist of stacked optically anisotropic thin-films with different optical functions. The key layer is the LC-layer which combines electrical and optical functions. With its effect-specific and voltage-dependent molecular configuration it enables the conversion of electrical signals into optical

information. Passive optical elements such as color filters, optical retarder film(s), reflectors, etc. are stacked onto the LC-layer. The unique stacking nature of LCDs permits to optimize the performance of individual optical functions and to tune them to specific display applications without compromising other functions. Optical functions can be added or removed to improve or to tune display performance.

Each LC-configuration with its specific advantages and disadvantages requires different passive optical elements to render it operable as a display. To enable new display applications, novel optical elements as well as new LC-configurations are required to resolve problems which are, in some cases, as old as the LCD technology. An example is the viewing angle dependent contrast of the thirty-year-old twisted nematic (TN)-effect [1] which is the basis for 70% of today's LCDs. To increase the contrast of TN-LCDs at large angles of view, their broad off-state field of view was extended to their non-planar on-state by incorporating discotic optical retarder films into the first generation of flat desk top TN-LCDs monitors [2]. However, to further improve LCDs and to enable new types of displays requires novel optical aligning and thin-film technologies with a high degree of design flexibility that meet the numerous needs of the increasingly diverse display applications. We have shown that thin-film stacks of photo-aligned nematic liquid crystal polymer (LCPs) films with controllable uniaxiality in space render virtually any optical retarder configuration feasible [3 - 7].

The best overall display performance results when the on- and off-state of an LC-configuration – which determine display contrast – are optimized in parallel with the gray scale performance of its intermediate switching states. Because of the static nature of on- and off-state, effect-specific passive optical functional films can be used to improve contrast, whereas multi-domain LC-configurations remedy poor gray scale performance. Recently we have realized such a combination for the case of a vertically aligned nematic (VAN) LC-layer. The LC-layer is multi-domain patterned by photo-alignment and then combined with a novel, negative birefringent liquid crystal polymer (LCP) retarder thin-film which is also photo-aligned [4]. To optimize display contrast the retarder is designed to correct residual unwanted polarization states in its on- and off-state while

simultaneously remedying the inherent viewing angle deficiencies of the polarizers; whereas the multi-domain LC-configuration corrects the viewing angle dependency of intermediate switching states, i.e. of grey levels and color shifts. The result is a display with excellent contrast and with an ideally broad field of view under any driving condition; it's black state is superior even to crossed polarizers [4].

In the 1980s first attempts were made to induce molecular reorientation in the bulk of guest-host liquid crystal samples by exposing LCPs which comprised mainly azo guest molecules to linearly polarized light [8 - 10]. In the early 1990s two research groups showed that it is possible to align monomeric liquid crystals at surfaces not by mechanical means – such as via brushed display substrates – but with light; i.e. contact-free [11, 12]. The two groups followed two fundamentally different aligning strategies using linear polarized UV light. The first group presented *single-molecular* processes in azo-type guest-host systems [11] which realign LCs through optically induced cis-trans isomerization via molecular realignment [13], or via directional bleaching of polyimide layers [14]. The second, i.e. our own, group designed a *bi-molecular* photo-aligning process which we denoted linear photo-polymerization (LPP) [12, 15]. The LPP-process optically selects pairs of photo-sensitive molecules among an initially isotropic molecular distribution in a given (polarization) direction. The pairs photo-react and *simultaneously* cross-link such that the consequent anisotropic distribution of LPP-molecules which gives rise to LC-alignment is fixed in-situ [12, 15]. The LPP-photo-alignment process is inherently photo-stable [15], and we have shown that its symmetry enables simultaneous alignment *and* bias tilt angle generation in monomeric- as well as in polymeric liquid crystals (LCPs) [16]. Moreover, we have shown that LCP films can be aligned via the aligned surface of a *single* substrate of glass, silicon wafers, plastic, etc; i.e. LCP layers need not be sandwiched between two aligning substrates, such as in displays, to undergo alignment [3, 5, 7].

In the following the broadening effects of gray scale performance of photo-aligned dual-domain TN-LCDs are shown. Thin-film stacks of LPP-photo-aligned nematic liquid crystal polymer (LCPs) films on *single* substrates, with controllable uniaxiality in space, enable a plethora of novel optical functions,

such as wide-view films, optical compensation films, polarisation interference color filters or photo-aligned and photo-patterned linear polarizers. Novel LPP/LCP-optical thin-film configurations are presented.

## 2. LPP-Photo-Alignment and Molecular Functions

Fig.1 schematically depicts our LPP photo-aligning model [12, 16] for the case of two adjacent pairs of new endo cinnamic ester polymer LPP-molecules made in our laboratories.

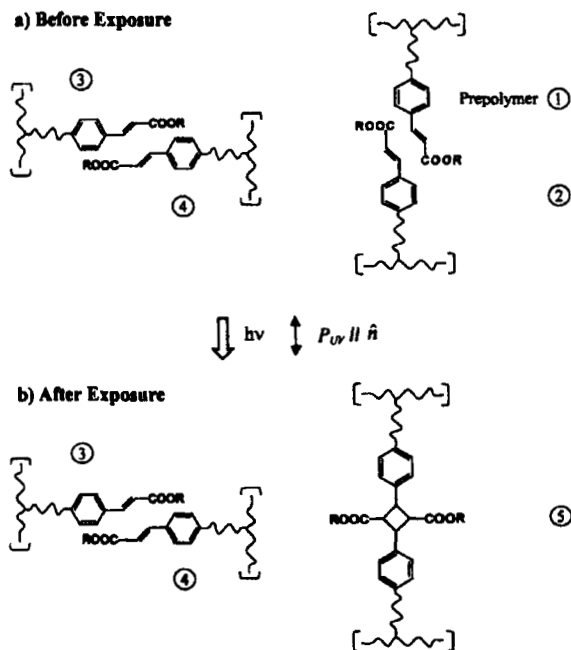


FIGURE 1 LPP photo-aligning model.

The pairs of LPP-molecules in the  $xy$ -plane are drawn to reflect the isotropic LPP distribution on the substrate prior to exposure of the LPP-layer to linearly polarized uv-light  $h\nu(P_{uv})$ ;

i.e. the number of polymer molecules along x-, y- (and z) direction are equal before polarized uv-exposure. The LPP-molecules are designed such that the 2+2 photo-reaction selectively cross-links adjacent, parallel pairs of LPP-molecules whose photo-sensitive transition moments happen to lie parallel to  $P_{uv}$ . In the LPP-process polarized uv-light induces (i) an anisotropic polymer distribution:  $1,2,3,4 \Rightarrow 3,4$ ; generates (ii) new molecules 5 which – due to directional cross-linking – are also anisotropically aligned; and finally (iii) simultaneously fixes the photo-generated anisotropic LPP-distribution via cross-linking. Fig.1 depicts the bi-molecular character of the LPP-process which stabilizes LPP-photo-alignment in-situ [12, 15]. Fig.1 also indicates the crucial, non-degenerate alignment symmetry of our LPP-process which differs from other photo-aligning mechanisms and which aligns the LC-director  $\hat{n}$  via Van der Waals interaction parallel to the polarization direction  $P_{uv}$ , thus enabling the generation of bias tilt angles in an adjacent LC-layer(s) by a single exposure step [16].

Since the beginning of today's LCD technology in the early 1970s, control of molecular alignment in field-effect LCDs was achieved by confining the LC-layer between two mechanically treated substrates. Because mechanical processes – such as buffing – are macroscopic, they are inadequate to generate azimuthal aligning patterns which are prerequisite to achieve multi-domain LCDs [17 - 22]. The LPP-photo-aligning process enables this goal, avoids substrate contamination and allows continuous display processing on glass- and plastic substrates [5, 12]. However, uniaxial photo-alignment, bias tilt generation and photo-patterning are not sufficient to realize high quality thin film transistor (TFT)-addressed, direct view LCDs, such as computer monitors, TV-sets, etc., or liquid crystals on silicon wafers (LCoS) for the micro-displays in projectors with their extremely demanding light stability requirements. Depending on the application, additional requirements have to be met by the aligning layer, such as induction of bias tilt angles  $\theta$  at display boundaries which preferably cover the boundary alignment requirements of all electro-optical effects from planar to homeotropic, i.e.  $0^\circ \leq \theta \leq 90^\circ$ ; azimuthal aligning anchoring strengths which are comparable to brushed polyimide; insolubility in LCs; voltage holding ratio  $HR > 95\%$  for TFT- and LCoS displays; thermally stable at temperatures  $T = 150^\circ$



during  $t = 2\text{h}$  (display processing time) and  $T = 120^\circ$  for  $t > 200\text{h}$ ; optically stable over the visible spectral range of  $420 - 700\text{nm}$  for light intensities  $I = 100\text{mW/cm}^2$  (sun-light) during  $t > 2000\text{h}$  for direct view LCDs, and  $I = 1\text{W/cm}^2$  for LCoS-displays; and last but not least: low uv-exposure aligning energies of  $20 - 60\text{ mJ/cm}^2$  at  $\lambda \approx 300\text{ nm}$  (fast alignment processing).

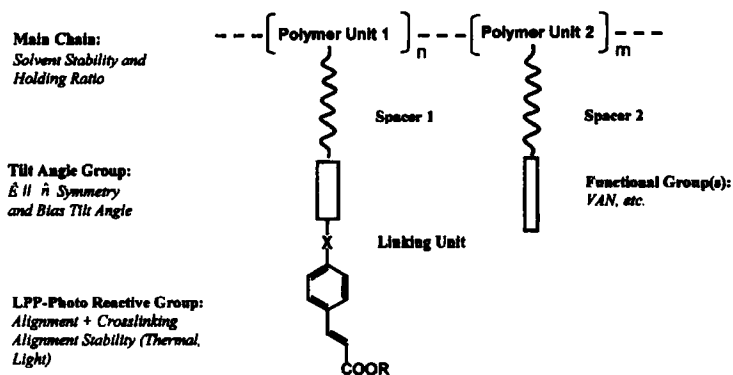


FIGURE 2 LPP side chain co-polymer concept: molecular functional entities.

To meet the above LC-photo-aligning goals we have identified specific functional molecular entities and correlated them with display performance. In a next step the entities were integrated into side-chain co-polymers such that the resulting LPP-polymers enable the above display properties. The resulting molecular building block design with functional entities permits to optimize different functions relatively independently of each other. Our LPP concept is schematically depicted in Fig. 2. The main chain polymer units 1 and 2 in Fig. 2 determine primarily LC-solubility and holding ratio HR. HR characterizes the capability of an aligning layer to getter residual ions in the LC-layer which leads to large specific LC-resistivities, thus preventing short-circuiting of TFTs [23]. Side chain 1 in Fig. 2 consists of functional groups which determine photo-sensitivity, cross-linkability, degree of non-centro-symmetry of the LPP-alignment process ( $\hat{n} \parallel P_{uv}$ ), and the range of (low) bias tilt

angles  $\theta$  for TN- and STN-LCDs. The second side chain in Fig. 2 enables large bias tilt angles  $\theta$  for photo-aligned VAN-LCDs.

### **3. Wide-View Displays: Multi-Domain TN versus LPP/LCP Wide-View Films**

The angular independent black-white contrast of an LCD monitor determines the legibility of displayed text under any angle of view, whereas angular independent reproduction of gray scale is prerequisite to properly display color and graphics information. Because of the voltage-dependence of the optical appearance of an LC-configuration, voltage-dependent optical deficiencies – such as angular dependent brightness – are best corrected for by voltage-dependent optical countermeasures, such as by multi-domain LC-configurations. Because the geometries of multi-domain LC-configurations do not change with temperature, they are ideal to improve gray scale performance of LCDs over a broad temperature range.

Because the on- or the off-state of a non-planar display configuration exhibits a restricted field of view, either state can be corrected and improved by adequate passive optical elements. In the following the effect on viewing angle dependency of contrast and brightness of single-domain versus dual-domain TN-LCDs are shown. LPP/LCP wide-view film compensation versus dual-domain photo-aligned display performance are compared.

Fig. 3 shows the well known viewing angle dependency of contrast and brightness of a single-domain TN-LCD operated in its first minimum. The angular dependent brightness is determined at 50% transmission at vertical light incidence. The display is LPP-photo-aligned. The azimuthal brightness dependence between the first and third quadrant in Fig. 3 shows the contrast inversion which occurs in uncompensated, partially switched, single-domain TN-LCDs. Also shown in Fig. 3 is the restricted field of view of its contrast (between on- and off-state).

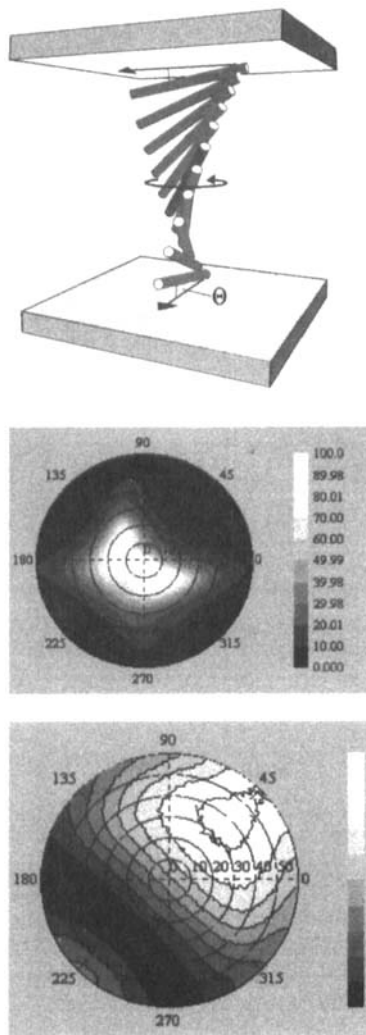


**FIGURE 3** Angular dependence of contrast (upper graph) and brightness (brightness adjusted for 50% transmission at vertical light incidence) of a single-domain TN-LCD; photo-aligned by ROLICs LPP-material JP 265.

See Color Plate I at the back of this issue.

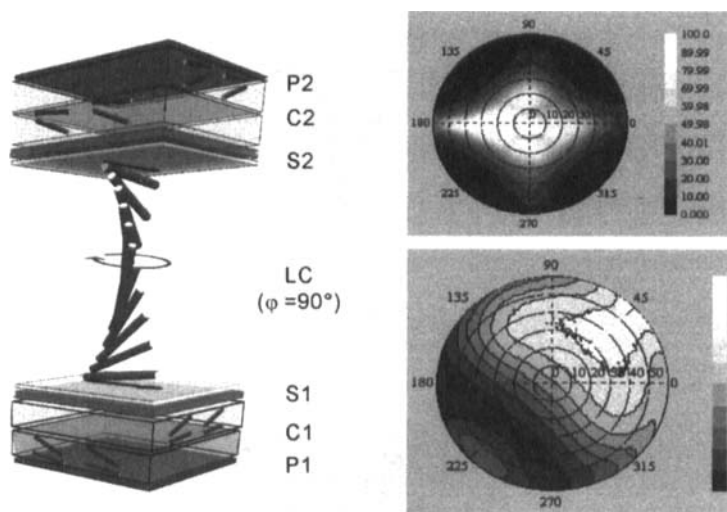


FIGURE 4 Angular dependence of contrast and brightness (brightness adjusted for 50% transmission at vertical light incidence) of photo-aligned single-domain TN-LCD which is optically compensated by LPP/LCP wide-view films. See Color Plate II at the back of this issue.

The transmission measurements of contrast and brightness depicted in Fig. 4 are made with the single-domain TN-LCD of Fig. 3 whose on-state is optically compensated by a pair of  $1.1 \mu\text{m}$  thin, nematic LPP/LCP film stacks  $C_1$  and  $C_2$ . The director configurations in each of the two crossed and tilted LCP-films  $C_1$  and  $C_2$  of Fig. 4 are chosen such that identical, negative birefringence results. They compensate the respective positive birefringence of the upper and lower tilted TN-LC-boundary layers in the on-state of the display without affecting its off-state (Fig. 4). The TN-wide-view films  $C_1$  and  $C_2$  of Fig. 4 are designed and made in our laboratories. From Fig. 4 and Fig. 3 it follows that LPP/LCP TN-wide-view films markedly reduce the viewing angle dependency of the contrast of single domain TN-LCDs. Moreover, they also slightly improve angular gray scale performance and do not exhibit any coloration under any viewing angle. Each of the two crossed LCP layers in  $C_1$  and  $C_2$  possesses an optical retardation of  $60\text{nm}$  and an average director

tilt angle of  $20^\circ$ . Like the TN-LCD, the LCP-films are LPP-photo-aligned such that the proper director tilt gradients result [7]. The respective total refractive indices of the two LCP layers are:  $n_x = n_y = 1.609$  and  $n_z = 1.571$ .

Fig. 5 shows the 50% transmission state of a LPP-photo-aligned and photo-patterned pixel of a dual-domain (2D)-TN-LCD [24]. Also shown are measurements of contrast and brightness versus angle of view of the display. The comparison of Fig. 5 with Figs. 3 and 4 shows that multi-domain alignment of LCDs remarkably broadens the field of view of the intermediate switching states and leads to uniform displays brightness. Combining multi-domain photo-alignment with wide-view film compensation remedies the viewing angle dependencies of the contrast as well as of the brightness of TN-LCDs [24].

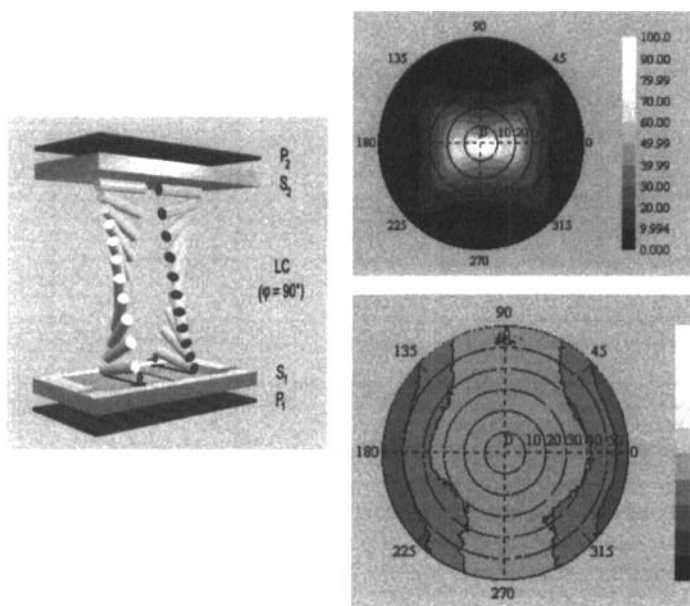


FIGURE 5 Angular dependence of contrast and brightness (50% transmission at vertical light incidence) of photo-patterned dual-domain TN-LCD.  
See Color Plate III at the back of this issue.

#### 4. Photo-aligned Polarization Interference Color Filters

Conventionally, interference color filters are made by sequential vacuum deposition of numerous layers of inorganic dielectric thin-films. We have shown that photo-alignment and photo-patterning of LPP/LCP-films enables novel polarization interference color filters which are made by spin coating, or by roll-to-roll wet-coating; i.e. by cost effective processes [3, 5, 6]. The LCP layers convert the photo-aligning information from the underlying LPP-layers into optical phase information [3]. LPP/LCP films are non-absorbing within the visible spectral range and therefore highly light stable.

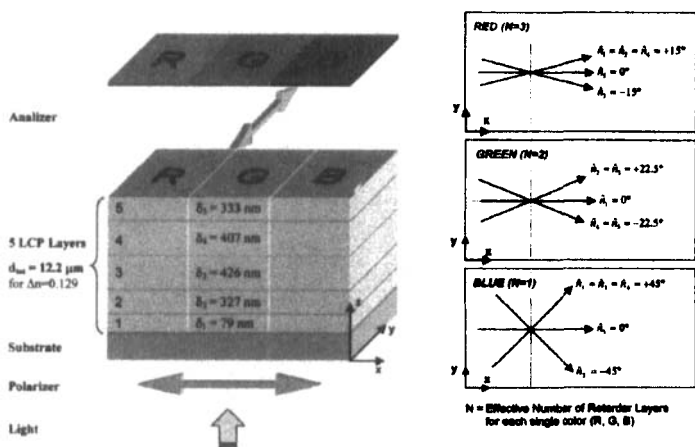
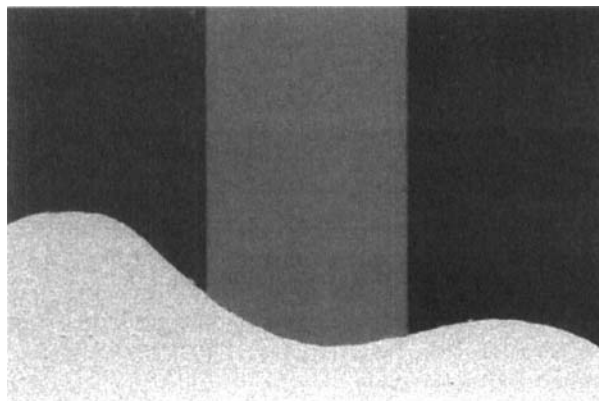


FIGURE 6 Geometry of a photo-aligned polarization interference color filter consisting of stacked LPP/LCP retarder films which generate the primary colors red (R), green (G) and blue (B) between crossed polarizers using ROLIC's LCP material CB 483.

The broad range of material parameters and the high degree of optical design flexibility of the LPP/LCP technology enable high quality polarization interference color filters with only few LPP/LCP layers. Fig.6 shows the geometry of a photo-patterned and photo-aligned stack of retarder films which

consists of only five LPP and LCP layers each and which generates the primary colors red, green and blue as well as the respective complementary colors when viewed in polarized light. The different azimuthal directions of the slow optical axes of the LCP layers and their thickness account for the different optical retardations required to generate the color coordinates R, G, B which meet PAL/SECAM standard [6]. The total thickness of the filter stack is  $12.3\ \mu\text{m}$  and its surface is flat.



**FIGURE 7** Photograph of a transmissive LPP/LCP polarization interference color filter according to Fig. 6 between crossed polarizer and analyzer. The white lower part of the filter is not covered by the analyzer.

See Color Plate IV at the back of this issue.

The upper part of Figure 7 shows a photograph of the LPP/LCP color filter of Fig. 6 between crossed polarizers  $P_1$  and  $P_2$  in transmission. The filter is illuminated by a white back light. The white area at the bottom in Fig. 7 is part of the filter which is not covered by the analyzer  $P_2$ ; it shows the virtually 100% transmission of the filter for unpolarized white light.

Figure 8 shows the red, green and blue transmission spectra of the color filter of Fig. 6 in the visible spectral range. The measurements are corrected for the wavelength dependent absorption of parallel polarizers. Taking into account 5% reflection losses at the two filter surfaces, it follows from Fig. 8 that LPP/LCP polarization interference color filters are virtually 100% transmissive over the visible spectral range. This renders

LPP/LCP filters/retarders ideal for all applications which require optimal brightness, such as portable displays, plastic LCDs, digital cameras as well as for applications where high light intensities occur, such as in the color management optics of projectors.

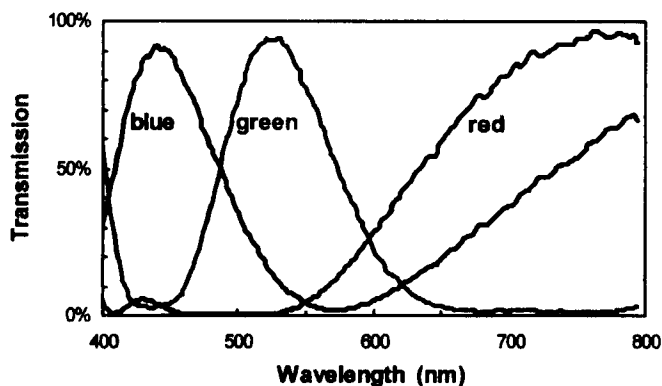


FIGURE 8 R,G,B transmission spectra of the color filter of Fig. 6 between crossed polarizers (100% transmission corresponds to parallel polarizers).

See Color Plate V at the back of this issue.

## 6. Photo-structured Linear Polarizers on Plastic Films

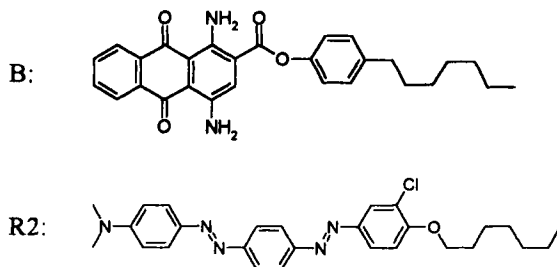
Iodine doped, polymer film based linear polarizers are mechanically stretched. Because of the super-cooled glass nature of polymers and despite high glass transition temperatures, stretched polymer films relax at elevated temperatures and lose their polarizing properties. In contrast to stretched polarizers, photo-aligned LPP/LCP films on single plastic- or glass substrates are not mechanically stressed. Therefore, they withstand temperatures up to 150°C in air for hundreds of hours [3]. Moreover, we have shown that LCP films can be photo-structured [3]. The combination of photo-alignment and photo-patterning of the alignment of nematic LPP/LCP thin-films therefore enables thermally highly stable linear polarizers with photo-patterned polarization directions when designing them as hosts for dichroic dyes. An application for photo-structured polarizers is the analyzer



in direct view stereo TN-LCDs. In the following we discuss the performance of the first photo-aligned LPP/LCP linear polarizers made on TAC (tri-acetyl-cellulose) plastic films.

Analogous to monomeric liquid crystals, nematic pre-polymer liquid crystals [25] can be doped with guest molecules which copy the local order of the nematic host. The order of the guest molecules can then be fixed by polymerization of the host; where the host order parameter  $S_{LC}$  is determined by the nematic-isotropic transition temperature  $T_c$  of the host [26] prior to polymerisation. The order  $S$  of the guest molecules depends not only on  $S_{LC}$  but also on the specific interactions between host and guest molecules. In the case of dichroic dyes, the dye order parameter  $S$  which scales with  $S_{LC}$  determines the extinction ratio for parallel and perpendicular linear polarized light. Because ideal order ( $S = 1$ ) cannot be reached in a surface aligned nematic matrix, the polarization ratio of LPP/LCP polarizers is smaller than that of stretched iodine polarizers. However, because of their large design and processing flexibility, LPP/LCP polarizers are promising new devices for many applications, such as for in-situ polarizers in future plastic LCDs.

The upper part of Fig. 9 shows measurements of the absorption spectra for parallel and perpendicular linear polarized light of four dichroic dyes in thin LCP layers which are photo-aligned on single TAC substrates. The four dyes Y (yellow), R1 (red 1), R2 (red 2) and B (blue) in Fig. 9 were made in our laboratories. They are selected such that uniform absorption results over the entire visible spectral range when incorporated into an LCP layer. The consequent linear polarizer appears black. The molecular structures of the dyes are similar to those which we designed in the 1980s for nematic guest host LCDs [27]. The structures of the blue (B) and the red (R2) dye are:



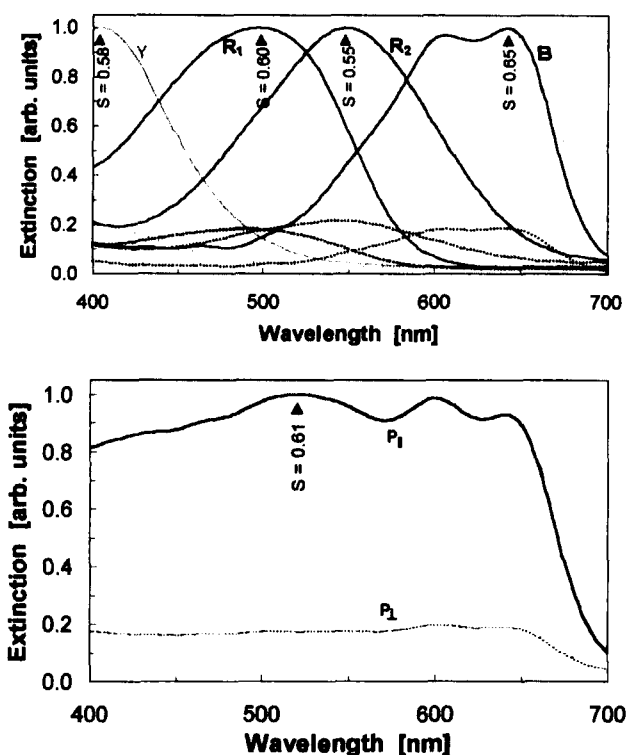


FIGURE 9 Upper graph: Absorption spectra for parallel and perpendicular polarized light of photo-aligned LPP/LCP dichroic linear polarizers on TAC substrates, each comprising the respective dichroic dyes Y (yellow), R1 (red), R2 (red) and B (blue). Lower Graph: Analogous absorption spectra of a 3 μm thin, black LPP/LCP dichroic linear polarizer on a TAC film comprising Y, R1, R2 and B.

See Color Plate VI at the back of this issue.

The lower graph of Fig. 9 shows the absorption spectra for parallel and perpendicular polarized light of a 3 μm thin, photo-aligned, black, LPP/LCP linear polarizer on a single TAC film comprising the four dyes of the upper graph of Fig. 9. From Fig. 9

and because of the rather large reduced temperature  $T/T_c = 0.874$  at which the LCP film was polymerized, relatively low dye order parameters  $S \approx 0.60$  result.  $S = 0.61$  corresponds to a polarization ratio of 5.71 (Fig. 9). However, increasing  $T_c$  of the LCP host and by tuning the molecular structures of the dyes to those of the LCP molecules should render photo-aligned polarizers with polarization ratios in excess of 15 feasible.



FIGURE 10 Photograph of a photo-aligned and photo-structured LPP/LCP dichroic guest-host linear polarizer image on a TAC film. The invisible part of the image on the left hand side of the picture is viewed in unpolarized light.

See Color Plate VII at the back of this issue.

We have shown before that photo-patterned alignment of LPP/LCP films on single substrates enables high resolution phase-retarder images with sub-micron resolution by a simple, two-step photo-aligning process [3, 28]. By photo-patterning the LPP-alignment layer via a digital photo mask prior to coating and polymerizing the above dichroic, black LPP/LCP guest-host LCP film, a photo-structured, black, linear polarizer results. The image depicted in Fig. 10 shows the first photo-structured LPP/LCP

guest-host polarizer on a TAC film with a resolution of 720 dpi (dots per inch). The polarization directions of the pixels are either parallel or perpendicular to the (uniaxial) analyzer through which the picture of Fig. 10 was taken. The (blank) part on the left of the photo-structured polarizer image of Fig. 10 is viewed in unpolarized light. Despite the rather low polarization ratio of only 5.7 of the structured polarizer image of Fig. 10, its optical quality is quite good.

## Conclusion

Photo-alignment and photo-patterning of the alignment of monomeric liquid crystals (LCs) at the two substrate boundaries of liquid crystal displays (LCDs) are shown to markedly improve gray-scale performance and brightness of the field of view of dual-domain TN-LCDs. The alignment requirements of different types of LCDs are shown to be met by a molecular building block design of linearly photo-polymerized (LPP) side-chain copolymers which enables optimization of different aligning parameters – such as bias tilt angle or anchoring energy – relatively independently of each other. Our extension of photo-alignment and photo-patterning from the monomeric LC-layers of displays – whose boundaries are aligned by *two* substrates – to photo-aligned polymeric liquid crystal (LCP) films on *single* aligned substrates is shown to broaden the field of the LPP/LCP technology remarkably. It enables novel optical thin film elements, such as colorless LPP/LCP wide-view films for any type of display, ideally bright polarisation interference color filters which meet PAL/SECAM color standards as well as photo-aligned dichroic linear polarizers. For TN-LCDs it is shown that multi-domain photo-alignment, combined with LPP/LCP wide-view films, renders optimal display contrast and brightness under any driving condition feasible. Apart from photo-aligned optical retarders, it is shown that LPP/LCP thin-films doped with dichroic dyes enable high resolution, photo-aligned and photo-structured linear polarizers on plastic films. The diverse examples of photo-aligned displays and novel optical thin-film elements illustrate the versatility of the LPP/LCP technology. The technology is equally well applicable to LCDs on glass-, CMOS- or plastic substrates. It permits to photo-align future plastic LCDs as well as to integrate the

required passive optical thin-film elements into the plastic substrates, such as polarizers, optical retarder elements, color filters and polarizers.

### Acknowledgments

It is my pleasure to acknowledge the fruitful discussions and the highly professional experimental support by Hubert Seiberle, Franco Moia and Richard Buchecker.

### References

- [1] M. Schadt and W. Helfrich, Swiss Patent no. 532 261 (1970); J. Appl. Phys. Lett. **18**, 127 (1971).
- [2] H. Mori, Y. Itoh, Y. Nishiura and Y. Shinagawa, SID Proc. Int. Display Workshop **IDW96**, 189 (1996).
- [3] M. Schadt, H. Seiberle, A. Schuster and S. Kelly, Jpn. J. Appl. Phys. **34**, 3240 (1995).
- [4] H. Seiberle, K. Schmitt and M. Schadt, SID Digest **Eurodisplay99**, 121 (1999).
- [5] J. Chen, K. C. Chang, J. DelPico, H. Seiberle and M. Schadt, Digest **SID99**, 98 (1999).
- [6] M. Schadt, H. Seiberle and F. Moia, SID Proc. Int. Display Workshop **IDW99**, 1013 (1999).
- [7] C. Benecke, H. Seiberle and M. Schadt, Jpn. J. Appl. Phys. **39**, 525 (2000).
- [8] M. Eich and J. H. Wendorff, Macromol. Chem. Rapid Commun. **8**, 467 (1987).
- [9] T. Todorov, L. Nikolova and N. Tomova, Appl. Optics **23**, 4309 (1984).
- [10] K. Ichimura, Y. Suzuki, T. Seki, A. Hosoki and K. Aoki, Langmuir **4**, 1214 (1988).
- [11] W. M. Gibbons, P. J. Shannon, S. T. Sun, B. J. Swetlin, Nature **351**, 49 (1991).
- [12] M. Schadt, K. Schmitt, V. Kozenkov and V. Chigrinov, Jpn. J. Appl. Phys. **31**, 2155 (1992).
- [13] J. Michl and E. W. Thulstrup, Spectroscopy with Polarized Light, VCH Publishers Inc., New York (1986).
- [14] J. Chen, D. L. Johnson and P.J. Bos, Phys. Rev. **54E**, 54 (1996).
- [15] M. Schadt and H. Seiberle, Digest **SID97**, 367 (1997).
- [16] M. Schadt, H. Seiberle and A. Schuster, Nature **381**, 212 (1996).
- [17] T. Sumita, Jpn. Patent Application 69960 (1977).
- [18] K. H. Yang, J. Appl. Phys. Lett. **31**, 1603 (1992).
- [19] K. Sumiyoshi, K. Takatori, Y. Hirai and S. J. Kaneko, J. SID **2/131** (1994).
- [20] Y. Kawata, K. Takatoh, M. Hasegawa and M. Sakamoto, Liq. Cryst. **16**, 1027 (1994).
- [21] T. Hashimoto, et al, Digest **SID95**, 877 (1995).
- [22] J. Chen, et al J. Appl. Phys. Lett. **67**, 1990 (1995).
- [23] M. Schadt, Ann. Rev. Mat. Sci. **27**, 305 (1997).
- [24] E. Hoffmann, H. Klausmann, E. Günter, P. M. Knoll, H. Seiberle and M. Schadt, Digest **SID98**, 734 (1998).
- [25] D. J. Broer, R. M. Hikmet and G. Challa, Makromol. Chem. **190**, 3201 (1989).
- [26] W. Maier and A. Saupe, Z. Naturforsch., Part A, **14**, 882 (1959).
- [27] M. Schadt and P. Gerber, Mol. Cryst. Liq. Cryst. **65**, 241 (1981).
- [28] F. Moia, H. Seiberle and M. Schadt, Proc. SPIE **3973**, 196 (2000).